Variable Speed and Ternary Units to Mitigate Wind and Solar Intermittent Production

Christophe NICOLET	Power Vision Engineering Sàrl, Ecublens, Switzerland
Antoine BEGUIN	Power Vision Engineering Sàrl, Ecublens, Switzerland
Basile KAWKABANI	EPFL Group of Electrical Machines, Lausanne, Switzerland
Yves PANNATIER	EPFL Group of Electrical Machines, Lausanne, Switzerland
Alexander SCHWERY	ALSTOM Renewable (Switzerland) Ltd, Birr, Switzerland
François AVELLAN	EPFL Laboratory for Hydraulic Machines, Lausanne, Switzerland

Abstract

This paper presents the modeling, simulation and transient analysis of the dynamic behavior of a mixed islanded power network of 1'850 MW including 1'300 MW of classical thermal power plant, 200 MW of wind power, 100 MW of photovoltaic installed capacity and a 250 MW pumped storage power plant. First, the modeling of each power plant is fully described. The model of the thermal power plants includes a high-pressure steam turbine and 2 low pressure steam turbines, the rotating inertias, and a 1'400 MVA turbo-generator with both power controller and voltage regulator. The 200 MW wind farm is modelled using an aggregated model of 100 wind turbines of 2 MW. The wind farm model comprises a stochastic model of wind evolution with wind gust, a power coefficient based model of wind turbine with a-priori controller and a synchronous generator with voltage regulator. The 100MW photovoltaic capacity is also modeled using an aggregated model. This model includes stochastic solar energy source, PV voltage source characteristic curve depending on both light intensity and PV system current, a-priori control system for maximum power tracking and voltage source inverter average model. Finally, the 250 MW pumped storage power plant model includes the head water reservoir, a 2'000 m gallery, a surge tank, the 900 m long penstock feeding the power unit connected to the downstream tank through a 250 m long tailrace water tunnel. For the power unit, two different technologies are considered: a 250 MW reversible pump-turbine with variable speed Doubly Fed Induction Machine, DFIM, and a ternary unit with Francis pump and turbine driving a fixed speed synchronous machine. The 4 power generation plants are connected to a passive consumer load via a 500 KV electrical line network. Then, the capability of the pumped storage plant to contribute to the islanded power network stability is investigated through the time domain simulation of the dynamic behavior of the entire mixed power network using the simulation software SIMSEN. The stability of the power network considering either the Variable speed unit or the Ternary unit, are compared with respect to frequency induced either by wind power fluctuations or PV output power fluctuations and in case of short-circuit.

1. Introduction

The installed capacity of new renewable energies, NRE, is constantly increasing worldwide since more than 20 years, and projections foresee a continuous growth of NRE at the horizon 2040 [33]. For example European Union targets a 20% share of electricity generation by renewable energies in 2020, a part of the so-called 20-20-20 energy policy, where wind and solar energies are expected to represent the main contribution to renewable energies generation increase. As illustrated in Figure 1, these two sources of energy are known for being highly volatile and therefore, their integration in the existing power networks will constitute a challenging task. This will require developing adequate primary, secondary and tertiary production reserves and massive storage capacities where pumped storage power plants should play a significant role [7]. Countries having very ambitious penetration rates of NRE, such as Portugal aiming

a share of 55% of the electricity generation by renewable energies by 2020, are also planning and developing large conventional and pumped storage capacities [18].

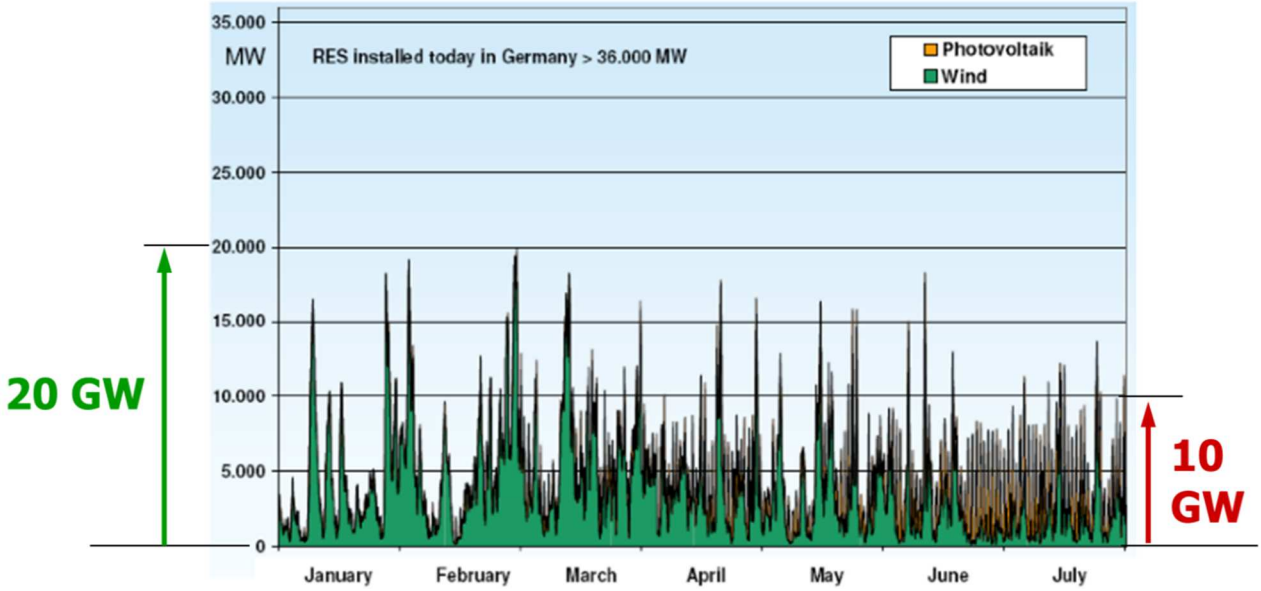

Figure 1 Wind and solar electricity generation in Germany in 2010 (adapted from: "A Comparison of Advanced Pumped Storage Equipment Drivers in the US and Europe" by R. K. Fisher et al., Hydrovision 2012, Louisville, USA.[7]).

Beside storage and substitution production capabilities, pumped storage power plants can also significantly improve the power network stability due to their production flexibility and ancillary services capabilities. However, the planning, design and optimization of new pumped storage power plant developed to compensate renewable energy volatility requires detailed analysis of the power network stability. In this context, advanced simulation models of each energy conversion power station are necessary to investigate the power network dynamic behavior and address the power network stability for various configurations and scenarios. This problematic is addressed in the present paper through the modeling, numerical simulations and analysis of the stability of a representative islanded power network case study of 1'850 MW capacity, depicted in Figure 2. This power network includes 1'300 MW of classical thermal power plant, 200 MW of wind power, 100 MW of solar power and 250 MW of hydropower. Apart from the hydro power, the ratio of renewable power to the total power is 11% and 5% for the wind and the solar plants respectively. The energy of the four power plants is transmitted to a passive consumer load via a 500 KV electrical line network as presented in Figure 2. For the pumped storage power plant, two different technologies are considered and compared: the ternary units and variable speed units based on doubly fed induction electrical machine.

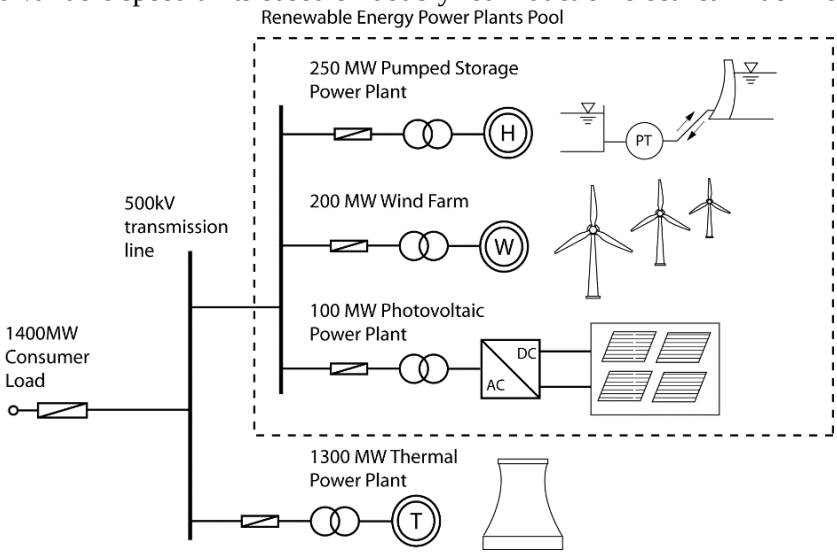

Figure 2 Case study power network.

2. Ternary units and variable speed technologies

The global design of pumped storage power plants can be fairly addressed considering the specific topology, the related hydrology, the power network location and related transmission issues, and environmental constraints. Then, the selection of the appropriate electromechanical equipment should take into account technical aspects such as efficiency, operating range, submergence, excavation volumes and related civil engineering work, maintenance and equipment lifetime, and the expected ancillary services. In this context, compared to classical reversible Francis pump-turbines operated at constant speed, ternary units and variable speed units offer various advantages, that have to be carefully evaluated for each project in order to select the most appropriate solution according to the power utility expectations [7], [14], [16], [31]. Regarding variable speed solutions two different technologies are possible: doubly fed induction machine (DFIM) and full power frequency converters (FPFC) coupled with synchronous motor-generators. Hildinger and Kodding [11] provided a detailed comparison of these two technologies also pointing out the technico-economical threshold between the DFIM and the FPFC solution currently set around 100 MW; FPFC being the most cost-effective solution for the lowest power and the DFIM being more cost effective solution for the higher power ratings. The present paper focuses on DFIM variable speed and ternary unit's solutions illustrated in Figure 3 for two pumped storage power plants currently under construction in Switzerland. The advantages and disadvantages of these two technologies compared to a classical reversible Francis pump-turbine are summarized in Table 1.

During the selection process, if most of technical aspects can be reasonably evaluated, aspects related to system stability, regulating services and other ancillary benefits are more difficult to address. Moreover, Transmission System Operators, TSO, require demonstrating the capability of new units to withstand typical power network faults and to comply with Grid Codes. In this context, time domain simulation of the dynamic behavior of the full pumped storage power plant including hydraulic circuit, electrical installations, control system and power network provide very useful insights for decision making.

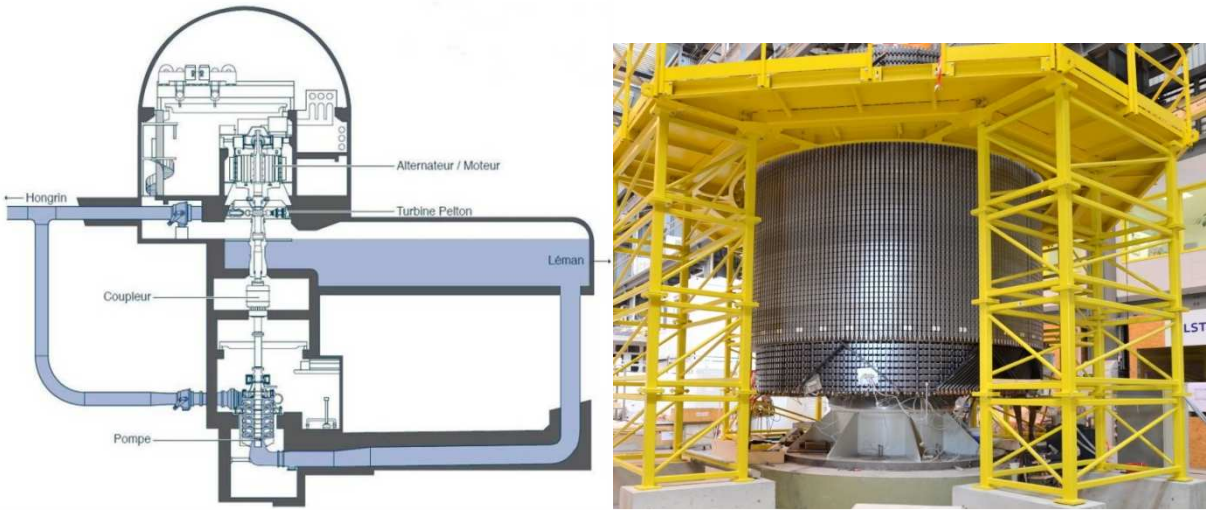

Figure 3 Example of 2 x 120 MW ternary unit of Forces Motrices de Hongrin Léman, FMHL, Pumped Storage power plant in Switzerland [10] (left), and rotor of the doubly fed induction machine motor-generator for 4 x 250 MW Linthal Pumped Storage Project in Switzerland on the right [28].

Table 1 Advantages and disadvantages of ternary units
and DFIM variable speed units compared to fixed speed reversible Francis pump-turbines.

	Ternary Units as compared to fixed speed pump-turbine [7], [10], [16], [31]	**DFIM Variable Speed Units as compared to fixed speed pump-turbine** [7], [8], [11], [13], [16], [17] [19], [23], [24], [25],[32]
Advantages	- High operational flexibility due to rapid change of operation mode from pump to turbine and vice-versa (same rotating direction) - Easy and short time start-up in pump mode (start-up with the turbine as drive) - Adjustable pump power in hydraulic short-circuit operation - Wide operating range in case of Pelton turbines - Increased efficiency in pump and turbine modes (optimal selection of the pump and turbine) - Proven technology - Smooth hydraulic transients	- Efficient active power control in pumping mode - Comply with large head variations - Higher efficiency in turbine mode - Extended operating range in turbine and pumping mode - Fast active power injection in pump and turbine mode due to “Flywheel” effect - Pump start-up without supplementary equipment - Reactive power control with Static Var Compensator even when the unit is at standstill
Disadvantages	- Higher investment costs (civil engineering due to total shaft line length and electromechanical equipment due to numerous components) - Higher maintenance due to electromechanical complexity and number of components - Increased ventilation losses in pumping mode due to turbine rotation - Lower efficiency in case of hydraulic-short circuit - Stability of the rotating train (long shaft) due to low pump submergence	- Higher investment costs (motor-generator and frequency converter, and related civil engineering) - Specific power limited for a given rotational speed - New technology

3. Case study description

The case study introduced in Figure 2, is investigated with the simulation software SIMSEN developed by EPFL, [26], [20]. Figure 4 presents the SIMSEN model of the case study including:

- 250 MW pumped storage power plant presented for the DFIM variable speed solution;
- 200 MW wind farm aggregated model;
- 100 MW photovoltaic power plant;
- 1'300 MW thermal power plant;
- 1'400 MW passive consumer load;
- all connected through a 500 kV transmission power network.

The modeling of each part of the case study is described in the following chapters.

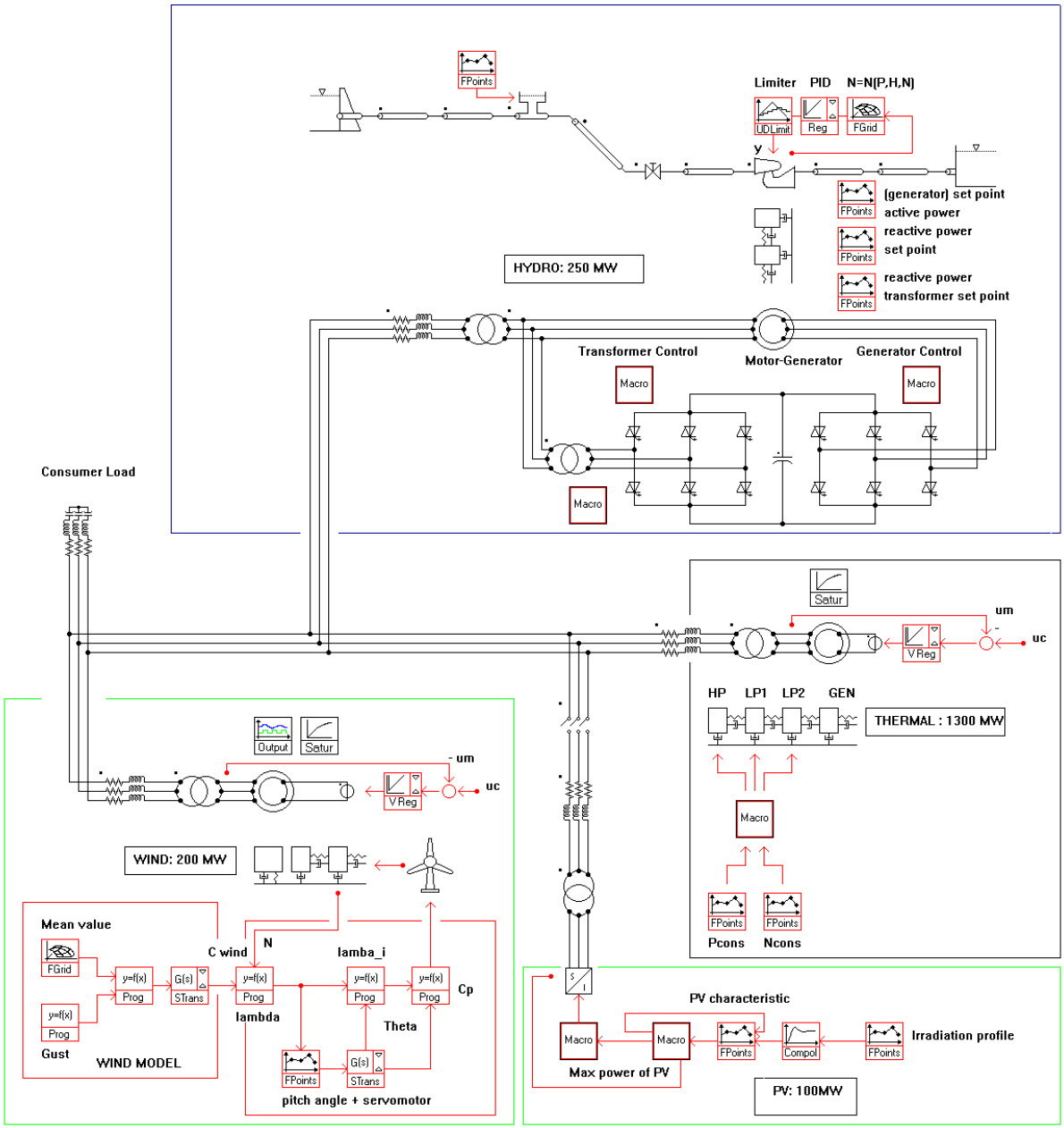

Figure 4 Islanded Power Network SIMSEN model with variable speed unit.

4. Hydraulic Power Plant Model

4.1. Ternary Unit Model

The layout of the hydraulic power plant is presented in Figure 5. The power plant is made of an upstream reservoir, a 1'950 m long gallery, a 885 m long penstock connected to a hydroelectric power house of +/-250 MW with a compound ternary machine type arrangement with fixed speed synchronous generator of 280 MVA, connected to the downstream reservoir by a tailrace water tunnel of 250 m long. Table 2 gives the main characteristics of the pumped-storage power plant. The hydraulic machines are modeled using their 4 quadrants hydraulic characteristics. The model of the piping system accounts for detailed water-hammer and mass oscillation phenomena [34], [20].

Table 2 Pumped-storage power plant characteristics.

Pump / Turbine	**Generator**
P_R = 250 MW	Rated apparent power: 280 MVA
N_R = 500 min^{-1}	Rated phase to phase voltage: 17.5kV
Q_R = 55 m^3/s	Frequency: 50 Hz
H_R = 510 m	Number of pairs of poles: 6
ν= 0.22	Stator windings: Y
$J_{pump\text{-}turbine}$=1.05 x 10^5 kg·m^2	J_{rotor}=8.1 x 10^5 kg·m^2

The model of the compound ternary units considered in this paper is presented in Figure 5. This model is composed of a Francis turbine of 250 MW, the synchronous generator of 280 MVA, a pump of 250 MW and a clutch between the generator and the pump. The turbine is equipped with a PID turbine speed and power governor with secondary control and the generator is controlled by standard voltage regulator. The model of the generator is based on an equivalent rotor circuit in the direct-axis and an equivalent rotor circuit in the quadrature-axis for taking into account the sub-transient behavior, see [4], [5].

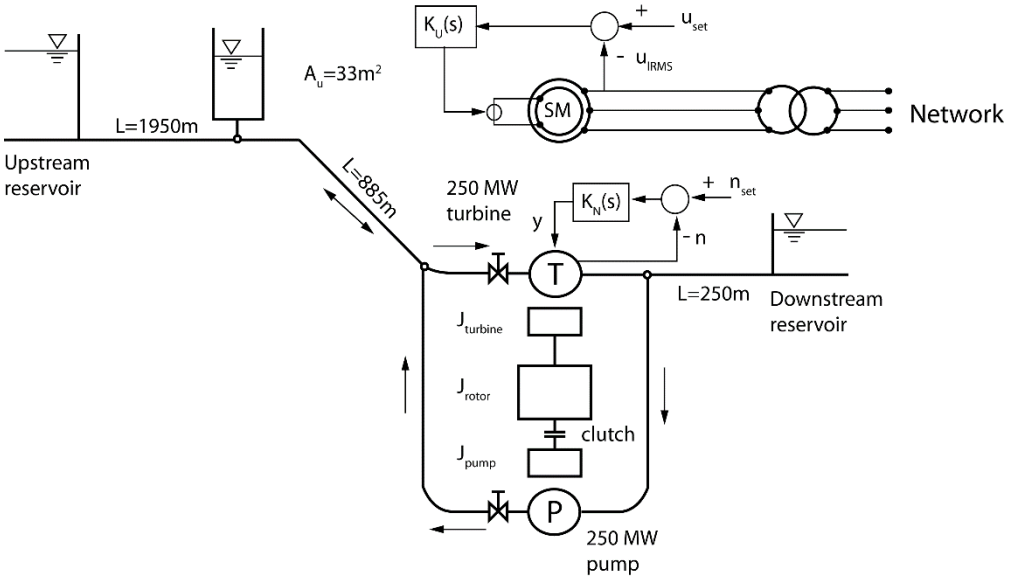

Figure 5 Pumped storage power plant model with fixed speed and 3 machine-type arrangements.

4.2. Doubly Fed Induction Machine (DFIM) Model

In the case of DFIM model the same hydraulic layout as the one of the ternary unit model is considered except for the hydraulic machine which is replaced by a reversible pump-turbine of 250 MW. The pump-turbine is driven using a speed optimizer which defines optimum speed in turbine mode and optimum guide vane opening in pump mode according to power and net head operating conditions, see [8], [13], [23]. The electrical system is made of a doubly fed induction motor-generator with 2 level VSI, Voltage Source Inverter, cascade in the rotor side. Large scale doubly fed induction machines, such as the one developed for the Linthal pumped storage project, see Figure 3 and [28], are in fact driven by 3 levels

VSI's contributing to reduce the voltage harmonics level. The model of the induction machine is based on classical d, q Park equations expressed in a, b, c quantities, [4].

This electrical system can be divided into two sections, a transformer section and a machine section, see Figure 6. The transformer section operates as a Static Var Compensator (SVC), its main role being to exchange reactive power with the grid. The reactive power and the capacitors voltage are controlled by acting on the transformer primary side currents through the right-side converter. The main role of the machine section is to control the active power of the machine. The active power and the stator reactive power of the machine are controlled by acting on the rotor currents through the left-side converter. The control structure of the transformer and machine sections can be found in [24].

As this hydropower plant is operating in islanded power network, a special care has been paid to set up the active power control structure in order to have fast response of the variable speed unit to network disturbances. Therefore, the active power set point of the DFIM accounts for network frequency deviations but also for power variation in the power network $\Delta P_{\text{network}}$, see [32]. This power variation is calculated as:

$$\Delta P_{\text{network}} = P_{\text{Load}} - P_{\text{set}_{\text{Therm.}}} - P_{\text{win}} - P_{\text{PV}} \quad (1)$$

This approach, also used to define the active power set point of the ternary unit secondary control, assumes that it is possible to measure the output power of the wind farm, the thermal power plant set point and the power consumption of the load. This approach is particularly relevant for small power networks with small number of producers and consumers and where the hydropower plant has a significant output capacity compared to the total power.

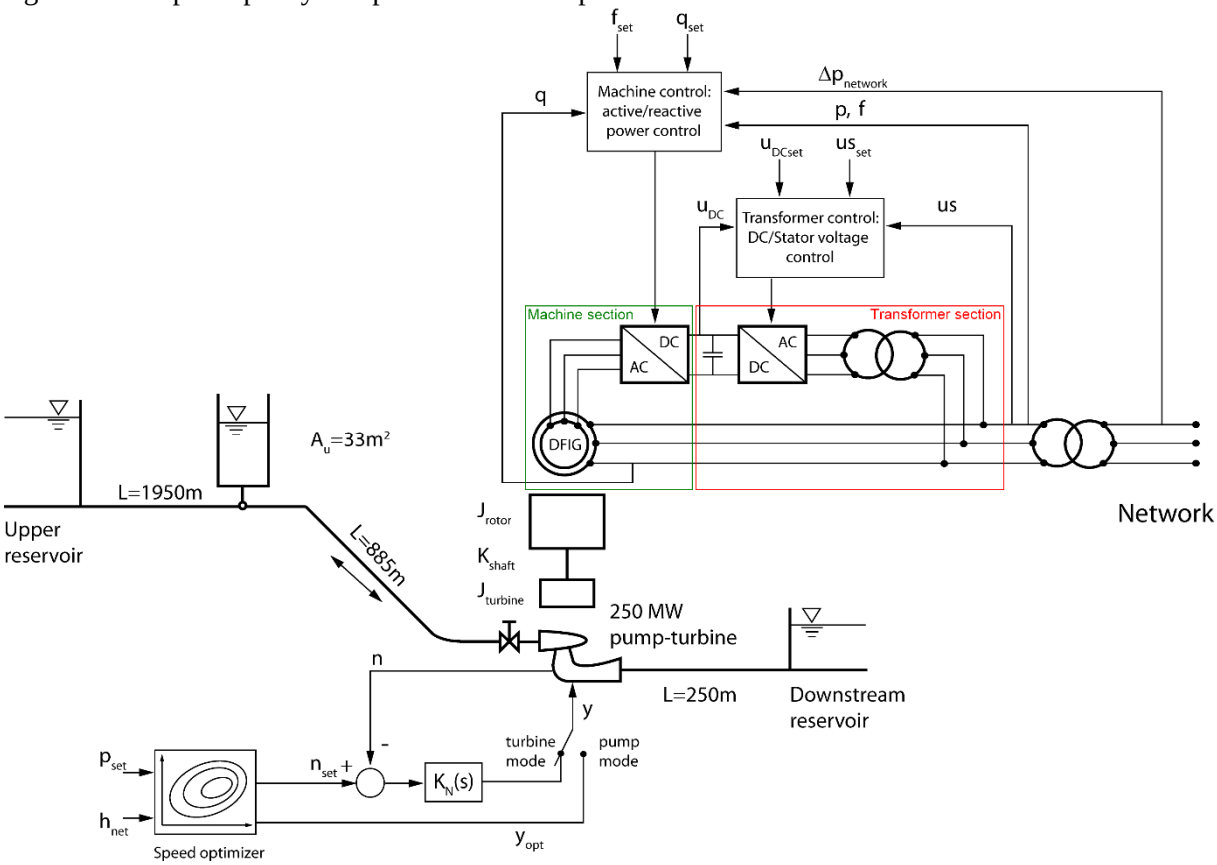

Figure 6 Pumped storage power plant model with variable speed pump-turbine.

5. Thermal Power Plant Model

The model of the 1.3 GW thermal power plant is based on steam flux and takes into account a constant pressure steam vessel, a regulating valve, a high pressure steam turbine, a steam transit through a re-heater and two low pressure steam turbines as presented in Figure 7. The model is based on valve and torque characteristics deduced from [2], on first order transfer functions for the turbine dynamics with τ_{HP}, τ_{LP} time constants, a re-heater modeled by a time delay b, and on a proportional regulator of constant Kp. The shaft line comprises 4 rotating inertias connected by 3 shafts with given stiffness and damping. And finally a turbo generator with 2 pairs of poles is also included in the model with a standard voltage regulator. The model of the generator is based on 2 equivalent rotor circuits in the direct-axis and 1 equivalent rotor circuit in the quadrature-axis considering saturation, leakage and damping effects of windings, allowing taking into account a sub-subtransient behavior, see [4], [5]. The parameters of the model are given in Table 3 and details of the model can be found in [21].

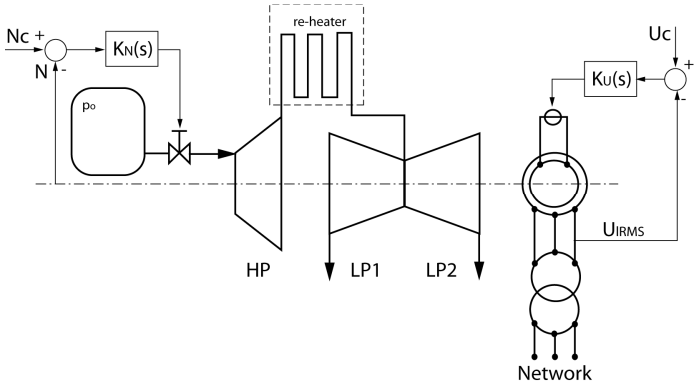

Figure 7 Thermal power plant model.

Table 3 Thermal power plant characteristics.

Steam turbines model	Mechanical masses inertias	Mechanical shaft stiffness and damping	Generator
τ_{HP} = 0.5 s τ_{LP} = 12 s b = 4 s Kp = 25	J_{HP} = 1.867 10^4kgm^2 J_{LP1} = 1.907 10^5kgm^2 J_{LP2} = 2.136 10^5 kgm^2 J_{GEN} = 5.223*10^4 kgm^2	K_1 = 3.614 10^8 Nm/rd K_2 = 8.206 10^8 Nm/rd K_3 = 4.116 10^8 Nm/rd μ_1 = 6.719 10^3 Nms/rd μ_2 = 7.06 10^3 Nms/rd μ_3 = 7.06 10^3 Nms/rd	Rated apparent power: 1400 MVA Rated phase to phase voltage: 28.5 kV Frequency: 50 Hz Number of pairs of poles: 2 Stator windings: Y

6. Wind Farm Model

6.1. Wind Turbine Model

The model of a 2 MW wind turbine is presented in Figure 8. It includes a model of the turbulent wind, the turbine with adjustable blade pitch angle θ and inertia J_{turbine}, the shaft stiffness k_{shaft}, the gear box, the synchronous generator of 2 MVA with voltage regulator and the transformer. The characteristics of the wind turbine model are given in Table 4. The model of the generator is based on 1 equivalent rotor circuit in the direct-axis and 1 equivalent rotor circuit in the quadrature-axis allowing taking into account a sub-transient behavior, see [4].

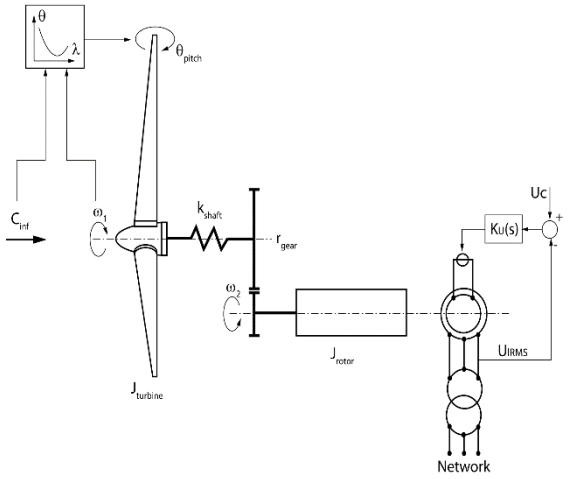

Figure 8 Wind turbine model.

Table 4 Wind turbine characteristics.

Operating datas	Wind turbine	Mechanical system	Generator
Cut-in wind velocity: 3.5 m/s Cut-out wind velocity: 20 m/s Rated wind velocity: 13 m/s	Number of blades: 3 Diameter: D = 75 m Rotational Speed: n_1 = 24.75 min^{-1}	r_{gear}= 3.032 k_{shaft} = 2.2 10^8 Nm/rd $J_{turbine}$= 3.15 10^6 kgm^2 J_{rotor}= 6.48 10^4 kgm^2	Rated apparent power: 2 MVA Rated phase to phase voltage: 400 V Frequency: 50 Hz Number of pairs of poles: 40 Stator windings: Y

The turbulent wind model is composed of a wind mean value and a wind gust, as suggested by Slootweg *et al.* [29]. The mechanical power transmitted by the fluid to the wind turbine can be expressed as:

$$P = \frac{1}{2}\rho \times A_{ref} \times Cp \times C_{\inf}^3 \quad (2)$$

Where A_{ref} is the swept area and C_p is the power coefficient and ρ is the air density. Heier [9] provides an empiric approximation of the wind turbine power coefficient C_p as function of the tip speed ratio λ is defined as:

$$\lambda = \frac{U_t}{C_{\inf}} = \frac{D_{ref} \times \omega_1}{2 \times C_{\inf}} \quad (3)$$

Where U_t is the blade tip velocity, C_{inf} is the wind velocity and ω_1 is the wind turbine rotating pulsation. Figure 9 left presents the power coefficient C_p of a wind turbine as function of the tip speed ratio λ and of the blade pitch angle θ obtained according to [9].

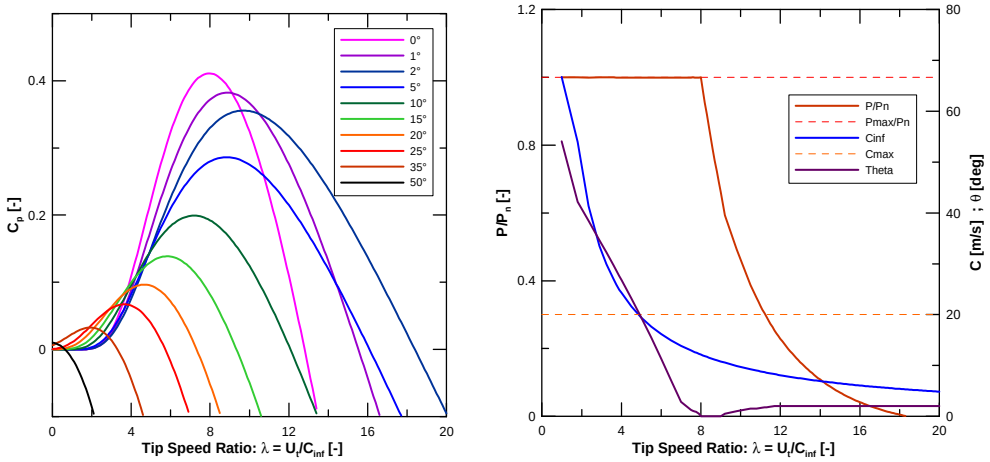

Figure 9 Wind turbine characteristic according to equation (4) (left) and wind turbine power, pitch angle and wind velocity and related limits as function of the tip speed ratio (right).

Then, the wind turbine output power is calculated from the characteristics given in Figure 9 left, as function of the tip speed ratio as presented in Figure 9 right, see also [30]. The blade pitch angle given as function of the tip speed ratio is also represented in Figure 9 right. For tip speed ratio above 8, the

pitch angle is selected to provide the highest power coefficient while below 8 it is selected to generate the 2 MW output power limit. The blade pitch angle θ is driven by a look-up table as function of the tip speed ratio λ as represented in Figure 9 right.

6.2. Aggregated Wind Farm model

For power grid stability purposes, it is possible to use an aggregated wind farm model, consisting of one wind turbine equivalent to *n* single wind turbines as presented in Figure 10, see [1]. Then, according to the energy conservation and in order to keep the same torsional mode eigenfrequency, the active power P_n, rotating inertias *J*, the shaft stiffness k_{shaft} and the swept area A_{ref} are multiplied by the number of wind turbines *n*. The parameters of the synchronous generator being given in per unit, they are kept constant.

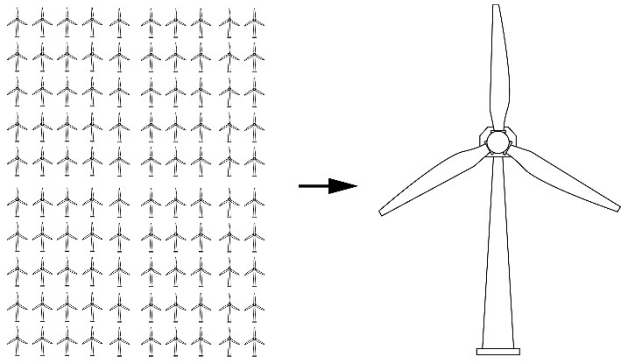

Figure 10 Wind turbine farm of 100 x 2 MW modeled as an equivalent wind turbine of 200 MW.

7. Photovoltaic Power Plant

In a photovoltaic power plant, the PV panels are arranged in series and parallel to build PV arrays of a given power. Each array is connected to its inverter which injects the DC harvested power into the AC grid. The maximum nominal power of such a block including PV array and inverter is mainly limited by the maximum common voltage of the PV panel and the turn-off capability of the inverter's power semi-conductors, current rating. Nowadays, a typical value of the block's maximal power is about 1 MW. Therefore it is necessary to parallel such blocks to achieve the rated PV plant capacity. For the network stability investigation presented in the present paper, it is not necessary to model each PV panel neither blocks. An equivalent PV plant, or aggregated model, consisting in one equivalent PV panel, one inverter and one transformer is often used [6]. A further simplification of the aggregated model is to represent the inverter with an average model which considers only the fundamental frequency of its output [6]. For this purpose, the inverter is reduced to a controlled three-phase voltage source, along with a simplified plant controller, see Figure 11 . The simplified model is divided into three groups: the equivalent PV source voltage-current, *U-I* characteristic, the PV plant controller and the physical elements including the three-phase voltage source, the transformer and point of common connection to the grid.

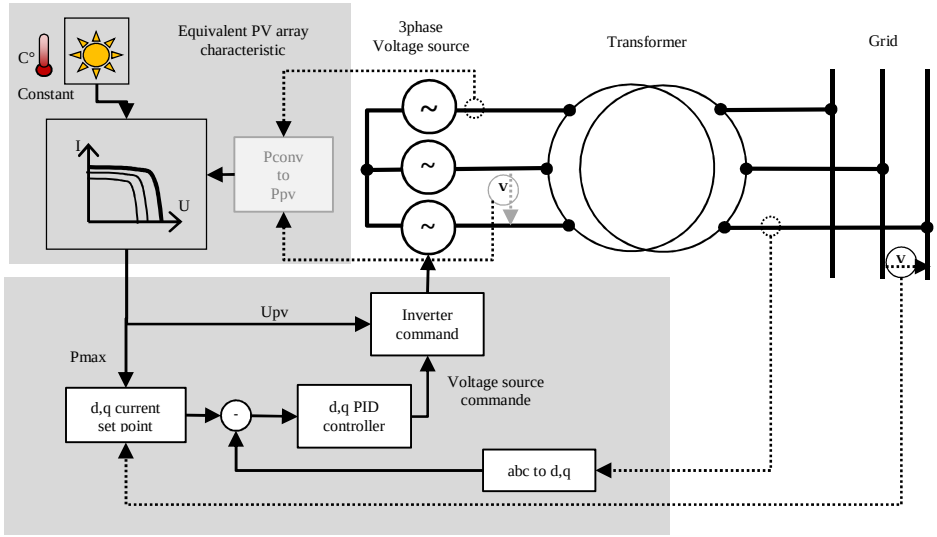

Figure 11 Pseudo-Continuous model of Photovoltaic power plant.

7.1. Equivalent PV source *U-I* characteristic

The static *U-I* characteristic of the equivalent PV source is a scaling of the characteristic of a single PV panel. Any degradation of the characteristic due to impedances of series and parallel connections is neglected. The *U-I* characteristic is implemented as an analytical algebraic relation according to [6], valid for a given solar irradiation.

$$I_{\mathrm{pv}} = f_{UI}\left(U_{\mathrm{pv}}, V_{\mathrm{max}}, I_{\mathrm{max}}, V_{\mathrm{oc}}, I_{\mathrm{sc}}\right)$$

with V_{max} and I_{max}, respectively the rated voltage and current operating point where maximum power is reached, and V_{oc} and I_{sc}, respectively the open circuit voltage the short circuit current for the rated irradiation. Those four parameters can be found in a data sheet of a PV panel and are often given for several values of solar irradiation and possibly for other cell temperature. In the model implemented here, those four parameters are linearly interpolated for values of irradiation between the set of values given by the data sheet. The maximum power (P_{pvMax}) that can be extracted from the PV source is simply the product $U_{\mathrm{max}} \times I_{\mathrm{max}}$. In the model of Figure 11, P_{pvMax} is then used as the power set point of the PV plant controller, multiplied by a representative value of the inverter's efficiency. Thus, the power set point of the plant controller is realistic and consistent with the PV sources and its weather conditions. This approach represents an ideal Maximum Power Point Tracking (MPPT) system. Table 5 gives the main numerical values of the simplified PV plant.

Table 5 Photovoltaic power plant characteristics.

PV panel	PV arrays	Aggregated model
Rated irradiation = 1000 W/m^2	$P_{ratedMax}$=1MW	N_{blocks}=100
U_{oc} = 60 V	N_{series} = 9	V_{oc}=5400 V
I_{sc} = 5.5A	$N_{parallel}$= 427	I_{sc}=23.4 kA
$U_{ratedMax}$=51 V @ 1000 W/m^2	V_{oc}=540 V	$U_{ratedMax}$=4590V
$I_{ratedMax}$= 5.1 A @ 1000 W/m^2	I_{sc}=2.34 kA	$I_{ratedMax}$ =21.8kA
$P_{ratedMax}$=260 W @ 1000 W/m^2	$U_{ratedMax}$=459V	Z_{rated}=21 m Ω
$U_{comMode}$=600V	$I_{ratedMax}$ =2.18kA	
Z_{rated}=10 Ω	Z_{rated}=21 m Ω	

7.2. Control of the PV plant

The inverter controller, via the inner current control loop, has the ability to control the amount of active power *P* and reactive power *Q* that are injected into the grid, at the point of common connection (PCC). By measuring the grid voltage RMS value, the power set point, coming from the equivalent PV source *U-I* characteristic, is translated into a current set point for the current controller. The PV plant can offer voltage support services to the network by injecting reactive current [6], however in the present study the solar plant is always operated with a unity power factor (Q = 0) at PCC. The inner current control loop is a simple d, q axis current control with proportional-integral (PI) controllers for both *d* and *q*

current components. The output of the current control gives the phase and magnitude of the three-phase voltage source. The current controller reacts to the variation of the DC voltage by adapting the modulation index accordingly automatically. However, in practice, this modulation index is limited and cannot compensate for any voltage drop on the DC side. To take into account the variation of the PV source voltage (U_{pv}), hence the DC side of the converter, the inverter's AC power is measured, via the three-phase current and voltage, and translated into a DC current that is the PV source current (I_{pv}) via the *U-I* characteristics. It is also possible here to take into account a theoretical converter efficiency. With this feedback on the PV source current, this simplified model can also represent unstable points when, after a sudden decrease of solar irradiation for example, the PV source enters an unstable point of operation, i.e $I_{pv}>I_{Max.}$ If the controller does not take appropriate action, the PV source will reach its short-circuit state. It is here the role of the MPPT system to detect such state and change *P* set point appropriately. The plant controller presented here is a simplification of a real one. The ideal MPPT is instantaneous and hence the set point of *P* is corrected quasi instantaneously also. Hence the PV source along with the current controller will not enter an unstable point, whereas a more realistic plant controller would have to deal with such unstable state. It is out of scope of the present study to have a model that manages this situation.

8. Transient Behavior of the Islanded Power Network

The transient behavior of the SIMSEN islanded power network of Figure 4 is simulated for the 3 following different load scenarios:

i) Photovoltaic sudden power variations;
ii) Wind power fluctuations;
iii) Short-circuit of 200 ms duration on the high voltage transmission system.

8.1. Initial load flow conditions

The initial conditions of the power flow of the islanded power network are summarized in Table 6. The thermal, wind and solar power plants are in generation operating conditions, close to rated output power while the consumer load is consuming 1'332 MW and the pumped storage plant is operated in pumping mode storing about 240 MW because of the excess of power production. The difference between the generation and consumption corresponds to the energy losses in transmission lines and transformers.

Table 6 Initial power flow.

Element	Active power *P*	Power flow
Hydropower Plant	240 MW	Consumption
Thermal Power Plant	-1'295 MW	Generation
Wind Farm	-189 MW	Generation
PV power plant (at PCC)	-100 MW	Generation
Consumer Load	1'332 MW	Consumption
Balance	12 MW	Lines and transformers Energy Losses

8.2. Sudden decrease of the solar irradiation

Figure 12 presents the time history of the solar irradiation and wind velocity considered for the first simulation scenario. The solar irradiation decreases from 1'000 W/m^2 down to 500 W/m^2 within 5 s, and then increases stepwise to its initial value. During this perturbation, the wind velocity is remaining constant at 14 m/s. Table 7 presents the simulation results obtained with the ternary units and with the DFIM variable speed unit considering the solar perturbation presented in Figure 12. The perturbation is corresponding to a power generation drop and increase of approximately 50 MW. The resulting power network frequency values are compared in Figure 13. The simulation results show :

- The ternary unit, which is operating in hydraulic-short circuit, is reducing its input power by increasing the turbine output power resulting from the turbine governor reaction to both the frequency drop and to the PV power plant output power drop;
- The variable speed unit constantly adapt its input power with the motor-generator control according to the renewable energy output fluctuations and also as function of the power network frequency; due to very fast reaction time, the pumped storage input power is able to follow the PV power plant power variations and thus is reducing the related frequency deviations;

– The comparison of the power network frequency values resulting from the PV generation variations shows that variable speed unit enables to reduce drastically the frequency deviations by a factor 10, compared to the results obtained with the ternary unit, with a maximum frequency deviation of 16mHz instead of 162mHz for the ternary unit;
– As presented in Figure 14, the total renewable power including photovoltaic, wind and hydro power remains constant at a mean value of 43 MW in the case of variable speed unit while it is decreasing down to 10 MW and increasing up to 85 MW for the case with ternary unit.

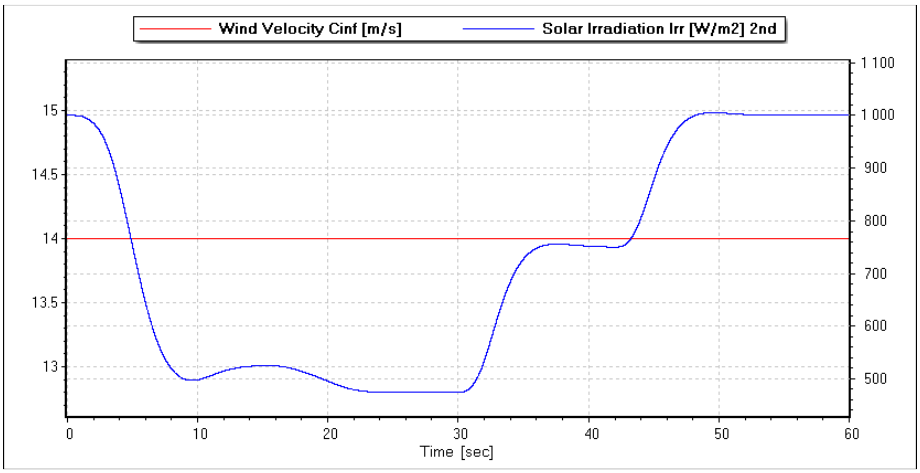

Figure 12 Solar Irradiation variation and wind velocity
during photovoltaic power plant output power sudden variations.

Table 7 Comparison of simulation results with Ternary Unit
and DFIM Variable Speed Unit in case of Photovoltaic sudden power variations.

	Ternary Unit	DFIM Variable Speed Unit
Power Plants Active Power	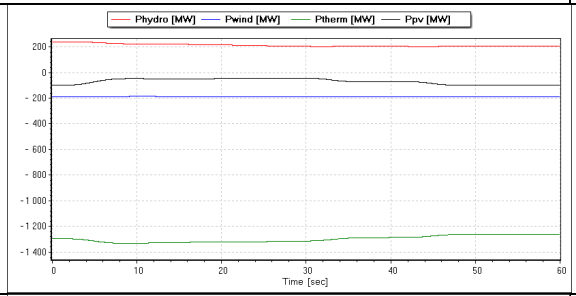	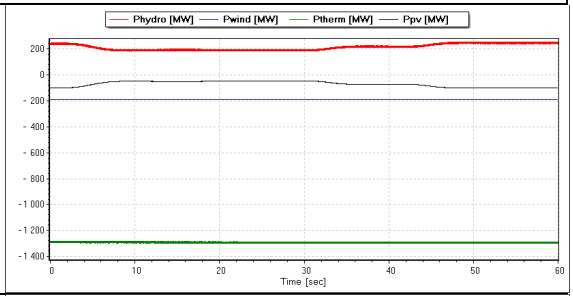
Pump Transient	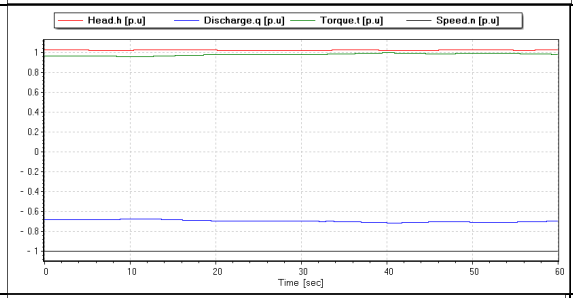	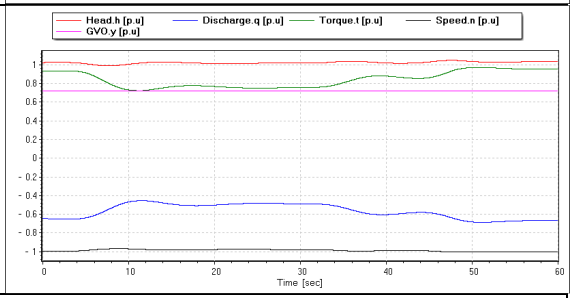
Turbine Transient (Ternary)	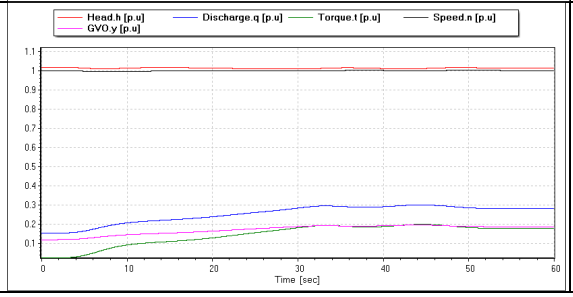	

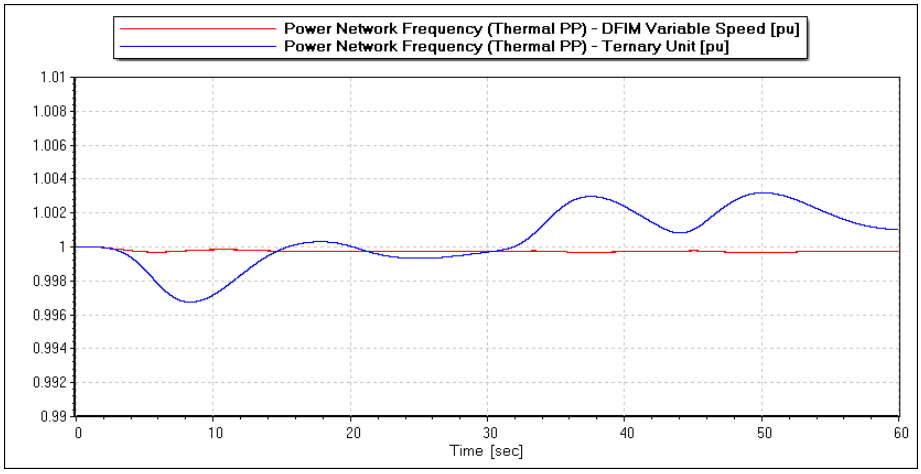

Figure 13 Comparison of the power network frequency resulting from photovoltaic power plant output power sudden variations of 50MW obtained with Ternary Unit and Variable Speed Unit.

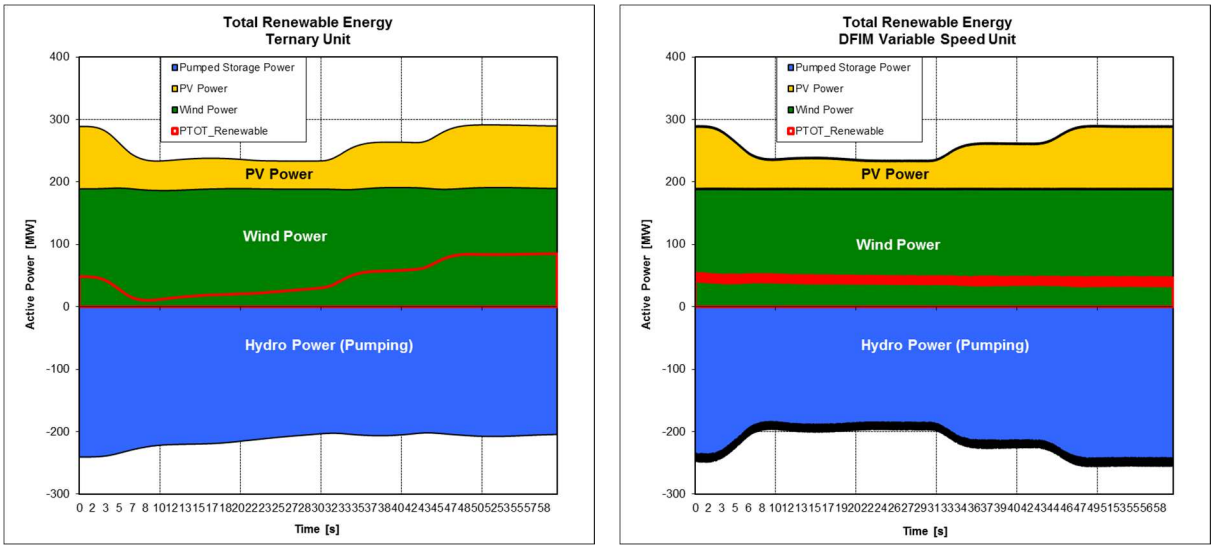

Figure 14 Comparison of the different renewable energy sources active power during photovoltaic power plant output power sudden variations of 50MW obtained with Ternary Unit (left) and Variable Speed Unit (right).

8.3. Wind power fluctuations

Figure 15 presents the time evolution of wind velocity around a mean value of 14 m/s considered for this second scenario, while the solar irradiation is considered constant at the value of 1'000 W/m^2. Figure **16** shows the corresponding wind power fluctuations and the resulting pumped storage input power variations. The frequency deviations obtained with ternary unit and variable speed unit are compared in Figure 17 pointing out frequency deviations reduced by a factor 5 with the variable speed unit compared to those obtained with the ternary unit.

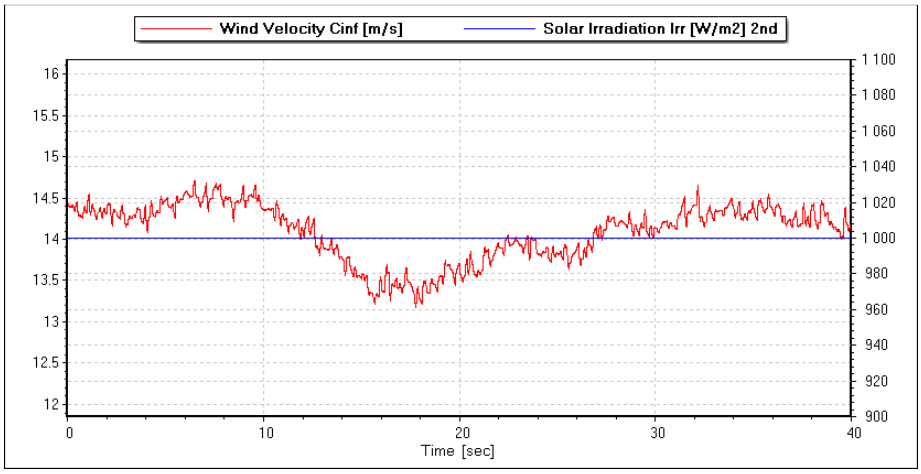

Figure 15 Wind velocity fluctuations and solar irradiation and during Wind Farm power plant output power fluctuations.

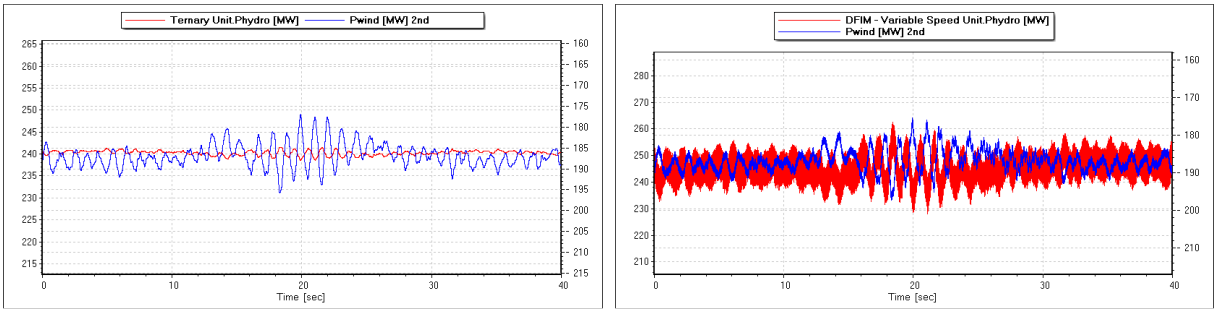

Figure 16 Comparison of the hydro power plant input power and wind farm output power resulting from wind velocity fluctuations obtained with Ternary Unit (left) and the Variable Speed Unit (right).

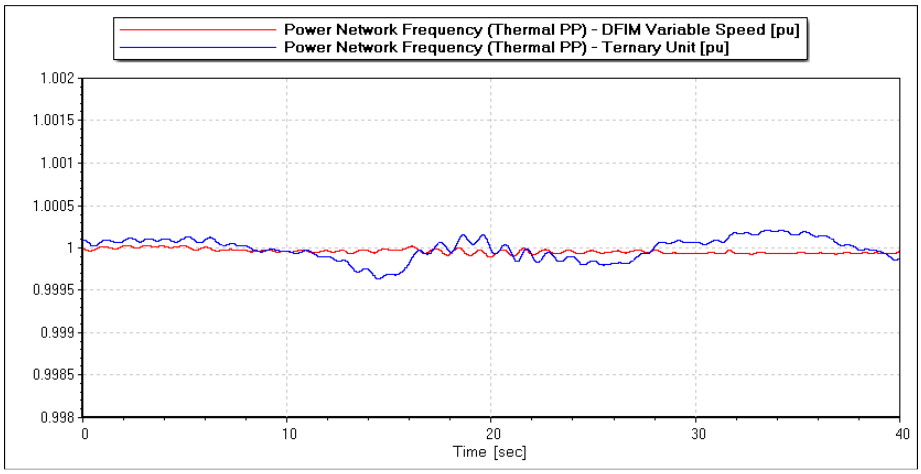

Figure 17 Comparison of the power network frequency resulting from Wind Farm power plant output power fluctuations obtained with Ternary Unit and Variable Speed Unit.

8.4. Stability in case of electrical short-circuit

Figure 18 presents the simulation result of the voltage RMS value of the consumer load obtained with the variable speed unit and resulting from a short-circuit on the high voltage transmission system at the pumped storage transformer terminals with a duration of 200 ms between t = 0.2 s and t = 0.4 s. This electrical fault is similar to the Fault Ride Through (FRT) capabilities which are specified in Grid Codes, [28]. The corresponding simulation results obtained with ternary unit and variable speed unit are presented in Table 8 and the resulting power network frequency values are compared in Figure 19.

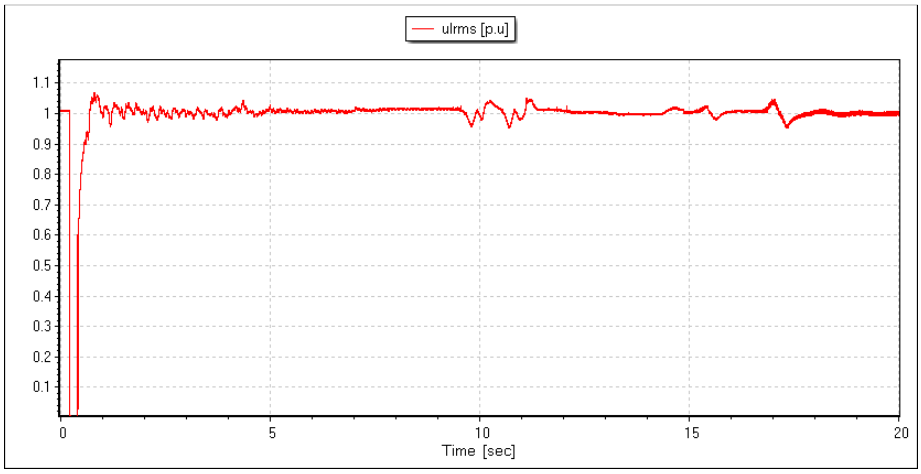

Figure 18 Consumer load voltage resulting from high voltage short-circuit of 200ms duration obtained with Variable Speed Unit.

Table 8 Comparison of simulation results with Ternary Unit and DFIM Variable Speed Unit in case of high voltage short-circuit of 200ms duration.

	Ternary Unit	DFIM Variable Speed Unit
Motor-Generator Transient	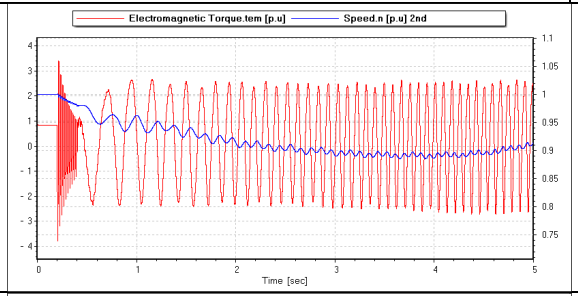	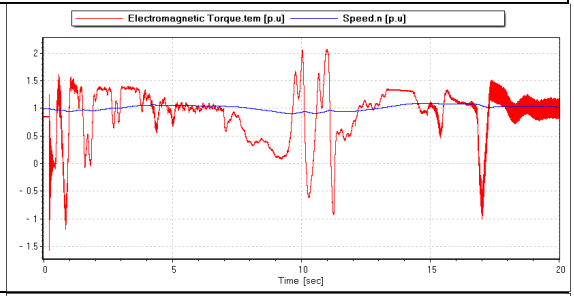
Pump Transient	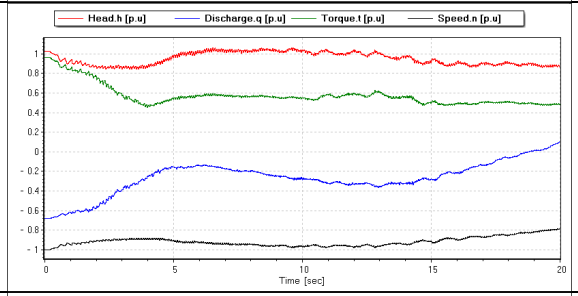	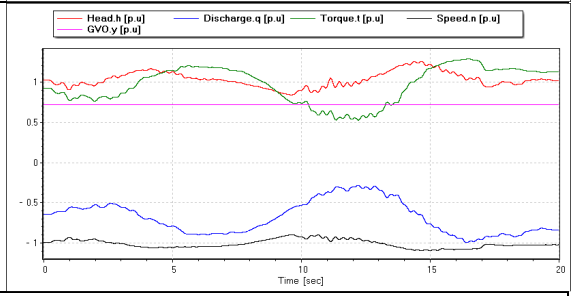
Turbine Transient (Ternary)	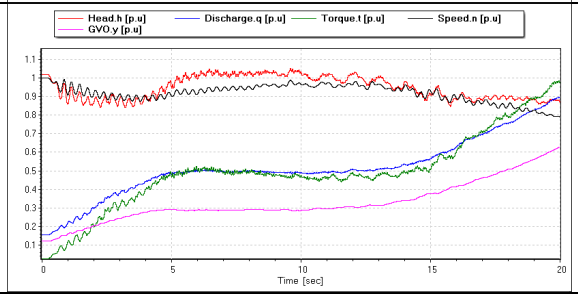	

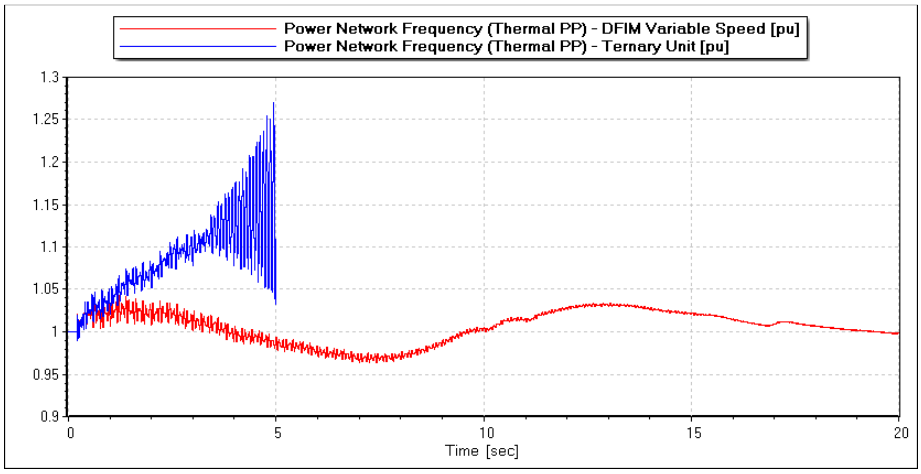

Figure 19 Comparison of the power network frequency resulting from high voltage short-circuit of 200 ms duration obtained with Ternary Unit and Variable Speed Unit.

The simulation results obtained with both technologies for the case of short-circuit of 200 ms duration on high voltage transmission system close to the consumer load, shows that:

- The ternary unit does not recover synchronism after the fault clearing, and as a consequence of the loss of the 240 MW input power in the power network, the power system frequency increases to 55 Hz in 2.5 s after the fault; the thermal power plant considered here as representative of the power network frequency, due to its large nominal power, also exhibits resonance phenomena due to over-frequency operation; as a consequence, the islanded power network would eventually experience a black-out in this specific configuration; the short-circuit duration should be reduced to 135ms to avoid the loss of synchronism of the ternary unit;
- Despite the strong electromagnetic torque fluctuations experienced by the variable speed unit, the unit features almost constant input power following the electrical fault, and as a consequence, the frequency of the power network remains around a mean value of 51.5Hz and is capable to recover stability after the fault clearance.

In the present case study, the islanded operation of the power network, represents detrimental conditions with respect to the pumped storage ability to remain in operation after the fault clearance when operating in pumping mode, compared to an interconnected operation mode. Indeed, during the short-circuit, the generating units increase their rotational speed as electromagnetic torques mean values are null, while the pumping units, decrease their rotational speed. As shown in Figure 20, this difference of rotational speed trend increases the difference of synchronisms between pumping units and generating units representative of the network frequency. As a consequence, the synchronism in pumping mode in islanded power network is lost for a shorter duration of short-circuit than in interconnected large grid where the grid frequency would remain almost constant.

The capacity of a hydro unit to withstand short-circuits or Low Voltage Ride Through specifications of grid codes represent a challenge, which depends on the selected technology, the power network configuration, and the unit operating mode, that requires to be addressed on a case by case basis.

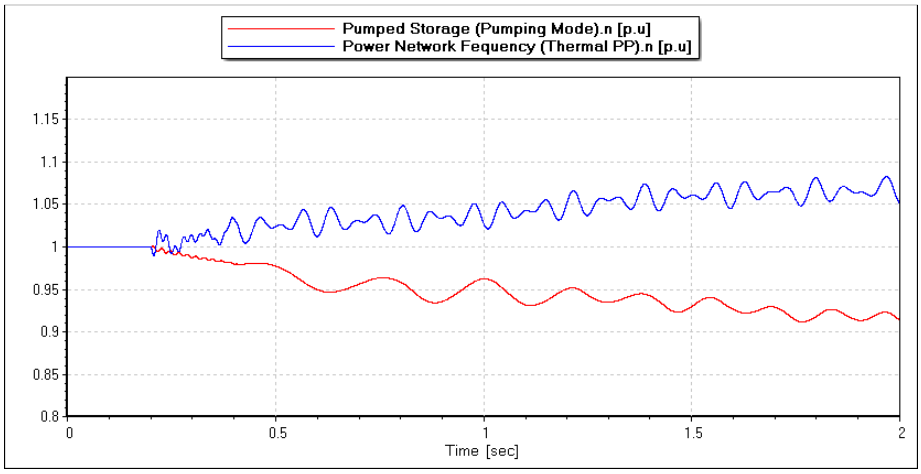

Figure 20 Comparison of the power network frequency, represented by the thermal power plant rotational speed, and the pumped storage rotational speed resulting from short-circuit of 200 ms obtained with in the case of Ternary Unit.

9. Conclusions

This paper is addressing the integration of new renewable energies together with pumped storage power plant by means of transient numerical simulations. The simulation results obtained for a mixed islanded power network in case of photovoltaic power variations, wind power fluctuations and short-circuits have shown that:

- Besides storage and substitution generation capabilities, pumped storage can also significantly contribute to power network stability due to their operating flexibility;
- Ternary units and variable speed units offer various advantages compared to classical fixed speed reversible pump-turbines, which have to be carefully evaluated according to the power network configuration with respect to its specific energy mix and load characteristics and also with respect to the transmission system requirements, i.e. the specific grid code [14];
- Numerical simulations of power network dynamic behavior based on realistic model of each production and consumption sources enable to compare quantitatively the contribution of different technical solutions to ancillary services and related system stability;
- The simulations results obtained with the variable speed unit have proven its high dynamic performances enabled by power electronics that drive the motor-generator and enable the “Flywheel” effect which can be decisive for islanded power network stability as shown in the case of short-circuits. Indeed, the variable speed unit features response time shorter than one second, due to power electronics, while, the ternary unit depending on hydraulic time constants, features response time of several seconds of order of magnitude.

The constant development of power electronics and the associated cost reduction yield new opportunities such as synchronous machine with Full Power Frequency Converter, offering even more flexibility such as direct transition from turbine to pump and vice-versa. The system dynamic simulations presented here, combined with operational cost simulations represent appropriate tools for the optimization of pumped storage power plants in view of a lean integration of intermittent New Renewable Energies.

10. Acknowledgments

The research leading to the results published in this paper is part of the HYPERBOLE research project, granted by the European Commission (ERC/FP7- ENERGY-2013-1-Grant 608532) [35] The authors also would like to gratefully thank ALSTOM Renewable (Switzerland) Ltd. in Birr, Switzerland and ALSTOM Renewable in Grenoble, France for their financial support and assistance in the framework of the EPFL Thesis N°4789 (2010) [25]. Granted by the CTI, Swiss Federal Commission for Technology and Innovation, (Grant No 8330).

11. Nomenclature

A: pipe cross section [m^2]
A_g: gallery cross section [m^2]
A_{ST}: surge tank cross section [m^2]
D_{ref}: machine reference diameter [m]
H: net head [m]
Q: discharge [m^3/s]
N: rotational speed [min^{-1}]
P: power [W]
l_g: length of the gallery [m]
p: pressure [Pa]
t: time [s]
x: position [m]
y: turbine guide vane opening [-]
Z: elevation above a datum [m]

T: Torque [Nm]
a: pipe wave speed [m/s]
h: piezometric head $h=z+p/(\rho g)$ [m]
g: gravity [m/s^2]
PCC: point of common connection
PV : photovoltaic
p: static pressure [Pa]

ν: specific speed
$\nu = \omega_R (Q_R / \pi)^{1/2} / (2 \cdot g \cdot H_R)^{3/4}$ [-]
ω: rotational pulsation [rd/s]
$_R$: subscript for rated

12. References

[1] Akhmatov, V., Knudsen, H, "An aggregate model of a grid-connected, large-scale, offshore wind farm for power stability investigations-importance of windmill mechanical system", Electrical power and Energy Systems 24, 2002.

[2] Bölcs, A., "Turbomachines thermiques", Vol. I, LTT/EPFL, 1993.

[3] Bucher, R., "Enhanced energy balancing and grid stabilisation through 3-machine-type variable-speed pumped-storage units", Proc. Int. Conf. Hydro 2007, Granada, Spain, October 2007.

[4] Canay, I. M., "Extended synchronous machine model for calculation of transient processes and stability", Electric machines and Electromechanics, vol. 1, pp. 137-150, 1977.

[5] Canay, I. M., "Physical significance of sub-subtransient quantities in dynamic behaviour of synchronous machines", Electric Power Applications, IEE Proceedings B (Volume:135 , Issue: 6), pp. 334-340, Nov. 1988.

[6] Delfino, F., Procopio, R., Rossi, M., Ronda, G.,"Integration of large-size photovoltaic systems into the distribution grids: a *P-Q* chart approach to asses reactive support capability",IET Renewable Power Generation, 2010, Vol. 4, Iss 4, pp 329-340.

[7] Fisher, R. K., et al., "A Comparison of Advanced Pumped Storage Equipment Drivers in the US and Europe", Louisville, USA, Hydrovision 2012.

[8] Grotenburg, K., Koch, F., Erlich, I., Bachmann, U., "Modeling and Dynamic Simulation of Variable Speed Pump Storage Unit Incorporated into the German Electric Power System", EPE 2001, Graz, Austria, 2001.

[9] Heier, S., "Grid integration of wind energy conversion systems", Chichester : Wiley, 1998.

[10] Herbivo, S. Laurier, P., Micoulet, G., Thackray, T.R., "Electromechanical equipment of FMHL and extension project of Veytaux Powerplant, Switzerland", Innsbruck, Hydro 2013.

[11] Hildinger T., Kodding, L., "Modern design for variable speed motor-generators-asynchronous (DFIM) and synchronous (SMFI) electric machinery options for pumped storage powerplants", Innsbruck, Hydro 2013.

[12] Hell J., Egretzberger M., Lechner A., Schürhuber R., Vaillant Y.: "Full size converter solutions for pumped storage plants – a promising new technology", Hydro2012, Euskalduna Congress Centre Bilbao, Spain, 29-31 October 2012.

[13] Kopf, E., Brausewetter, S., Giese, M., Moser, F., "Optimized control strategies for variable speed machines," In Proceeding of the 22nd IAHR Symposium on Hydraulic Machinery and Systems, Stockholm, Sweden, June –July 2004.

[14] Koutnik, J., Bruns, M., Meier, L., Nicolet, C., Pumped Storage - Grid Requirements For Behavior of Large Motorgenerators and Confirmation Of Compliance Through Simulation, Proceedings of HydroVision International, 19-22 July 2011, Sacramento, CA, USA, Session: Pumped Storage Design, Technology and Operation, pp. 1-11.

[15] Koutnik, J., Foust, J., Nicolet, C., Saiju, R., Kawkabani, B., Pump-Storage Integration with Renewables – Meeting the Needs Using Various Concepts, Proceedings of HydroVision International, 27-30 July 2010, Charlotte, NC, USA, Session: Pumped-Storage Market Trends and Strategies, paper 5, pp. 1-12.

[16] Koritarov, V., "Modeling and Analysis of Value of Pumped Storage Hydro", NHA Annual Conference 2013, Washington, DC, USA. http://www.dis.anl.gov/psh

[17] Kuwabara, T., Shibuya, A., Furuta, H., Kita, E., Mitsuhashi, K., "Design and Dynamic Response Characteristics of 400 MW Adjustable Speed Pumped Storage Unit for Ohkawachi Power Station", IEEE Transactions on Energy Conversion, vol. 11, issue 2, pp. 376-384, June 1996.

[18] Martins, N., et al., “The integration of large amounts of renewable energy in the Portuguese Power System”, SHF : «Pumped storage Powerplants», Lyon, nov. 2011.

[19] Mohan, N., Undeland, T.M., Robbins, W. P., “Power Elecronics, Converters, Applications and Design”, John Wiley & Sons, 2003

[20] Nicolet, C., “Hydroacoustic modeling and numerical simulation of unsteady operation of hydroelectric systems”, Thesis EPFL n° 3751, 2007, (http://library.epfl.ch/theses/?nr=3751).

[21] Nicolet, C., Greiveldinger, B., Hérou, J.-J., Kawkabani, B., Allenbach, P., Simond, J.-J., Avellan, F**.,** “High Order Modeling of Hydraulic Power Plant in Islanded Power Network”, IEEE Transactions on Power Systems, Vol. 22, Number 4, November 2007, pp.: 1870-1881.

[22] Nicolet, C., Pannatier, Y., Kawkabani, B., Schwery, A., Avellan, F., Simond, J.-J., "Benefits of Variable Speed Pumped Storage Units in Mixed Islanded Power Network during Transient Operation", Proceedings of HYDRO 2009, in Lyon, France.

[23] Pannatier, Y., Nicolet, C., Kawkabani, B., Simond, J.-J., Allenbach, Ph., “Dynamic Behavior of a 2 Variable Speed Pump-Turbine Power Plant”, ICEM 2008, XVIII International Conference on Electrical Machines, Vilamoura, Portugal, September 2008.

[24] Pannatier, Y., Kawkabani, B., Nicolet, C., Simond, J.-J., Schwery, A., Allenbach, P., Investigation of control strategies for variable speed pump-turbine units by using a simplified model of the converters, IEEE Transactions on Industrial Electronics, Volume: 57, Issue: 9, 2010, pp: 3039-3049.

[25] Pannatier, Y., Optimisation des strategies de réglage d’une installation de pompage-turbinage à vitesse variable, Thesis EPFL n° 4789, 2010, (http://library.epfl.ch/theses/?nr=4789).

[26] Sapin, A., “Logiciel modulaire pour la simulation et l’étude des systèmes d’entraînement et des réseaux électriques”, Thesis EPFL n° 1346, 1995, (http://library.epfl.ch/theses/?nr=1346).

[27] Schlunegger, H., Thöni, A., “100MW full-site converter in the Grimsel 2 pumped-storage plant”, Innsbruck, Hydro 2013.

[28] Schwery, A., Kunz, T., Gökhan, S., “Adjustable speed pumped storage plants – Innovation challenges and feedback of experience from recent projects”, Hydrovision International, Louisville, KY, USA, 2012.

[29] Slootweg, J. G. , De Haan, S. W. H., Polinder, H., Kling, W. L., “General model for representing variable speed wind turbines in power system dynamics simulations”, IEEE Transactions On Power Systems, Vol. 18, No. 1, February 2003.

[30] Slootweg J.G., Polinder H., Kling W.L., “Representing wind turbines electrical generating systems in fundamental frequency simulations”, IEEE Transactions on energy conversion, VOL. 18, NO. 4, 2003.

[31] Spitzer, F., Penninger, G., “Pumped storage power plants – Different solutions for improved Ancillary services through rapid response to power needs”, Hydrovision 2008, Sacramento, USA, July 14-18, 2008, paper 180.

[32] Suul, J. A., Uhlen, K., Undeland, T., “Variable speed pumped storage hydropopwer for integration of wind energy in isolated grids”, IEEE, NORPIE/2008, Nordic Workshop on Power and Industrial Electronics, June 9-11, 2008.

[33] U.S. Energy Information Administration, “International Energy Outlook (IEO) 2013”, DOE/EIA-0484 (2013), July 2013. http://205.254.135.7/forecasts/ieo/pdf/0484(2013).pdf

[34] Wylie, E. B. & Streeter, V.L., “Fluid transients in systems”. Prentice Hall, Englewood Cliffs, N.J, 1993.

[35] https://hyperbole.epfl.ch

The Authors

Dr. Christophe NICOLET graduated from the Ecole polytechnique fédérale de Lausanne, EPFL, in Switzerland, and received his Master degree in Mechanical Engineering in 2001. He obtained his PhD in 2007 from the same institution in the Laboratory for Hydraulic Machines. Since, he is managing director and principal consultant of Power Vision Engineering Sàrl in Ecublens, Switzerland, a company active in the field of optimization of hydropower operation. He is also lecturer at EPFL in the field of "Transient Flow in Systems".

Dr. Antoine BEGUIN graduated from the Ecole polytechnique fédérale de Lausanne, EPFL, in Switzerland, and received his Master degree in Electrical Engineering in 2006. He obtained his PhD in 2011 from the same institution in the Laboratory for Power Electronics in the field of Poly-phased Matrix Converter development and optimisation. Since, he is working with Power Vision Engineering Sàrl in Ecublens, Switzerland.

Dr. Basile KAWKABANI received his master degree in 1978 from SUPELEC, Ecole Supérieure d'Electricité in Paris France, and his PhD degree in 1984 in Electrical Engineering from the Ecole polytechnique fédérale de Lausanne, EPFL, in Switzerland. From 1992 to 2010, he was lecturer and research associate at the EPFL Electrical Machinery Laboratory. He is currently a senior scientist in STI Scientists Group (Electrical Machinery - EPFL), and senior member of the IEEE. His interests include modeling of power systems, power system stability and control.

Dr. Yves PANNATIER graduated from the EPFL and received his Master degree in Electrical Engineering in 2007. He obtained his PhD in 2010 from the same institution in the Laboratory of Electrical Machines in the field of simulation of variable speed units in transient operation. Since, he is working with Hydro Exploitation SA in Sion, Switzerland.

Dr. Alexander SCHWERY holds a PhD degree in Electrical Engineering from the Swiss Federal Institute of Technology (EPFL 1999) in Lausanne. He joined ALSTOM (Switzerland) Ltd. in 1999 were his main field of activity was the use and development of different simulation and calculation tools for salient pole generators. Between 2002 and 2011 Alexander was leading the Electrical and Ventilation group in the Technology Center in Birr, Switzerland. In 2011 he has been appointed Director R&D Electrical, in this function he has the overall responsibility for the Electrical R&D in Alstom Hydro.

Prof. François AVELLAN graduated in Hydraulic Engineering from INPG, Ecole Nationale Supérieure d'Hydraulique, Grenoble France, in 1977 and, in 1980, got his doctoral degree in engineering from University of Aix-Marseille II, France. Research associate at EPFL in 1980, he is director of the Laboratory for Hydraulic Machines since 1994 and was appointed Ordinary Professor in 2003. From 2002 to 2012, Prof. F. Avellan was Chair of the IAHR Committee on Hydraulic Machinery and Systems and he is convenor of the IEC TC4 Maintenance Team MT32 of IEC 60193 standard.